Physics of Fluids

Exact time scale of energy exchange in triad interactions of homogeneous isotropic turbulence

Cite as: Phys. Fluids **33**, 035136 (2021); https://doi.org/10.1063/5.0041020
Submitted: 18 December 2020 • Accepted: 09 February 2021 • Published Online: 12 March 2021

T. Wu (吴彤), **L. Fang** (方乐) and **Z. Wang** (王展)

Physics of Fluids ARTICLE scitation.org/journal/phf

Exact time scale of energy exchange in triad interactions of homogeneous isotropic turbulence

Cite as: Phys. Fluids **33**, 035136 (2021); doi: 10.1063/5.0041020
Submitted: 18 December 2020 · Accepted: 9 February 2021 ·
Published Online: 12 March 2021

T. Wu (吴彤),[1] L. Fang (方乐),[1,2,a)] and Z. Wang (王展)[3]

AFFILIATIONS

[1]LMP, Ecole Centrale de Pékin, Beihang University, Beijing 100191, China
[2]Beihang Hangzhou Institute for Innovation at Yuhang, Yuhang 310000, Hangzhou, China
[3]Institute of Mechanics, Chinese Academy of Sciences, Beijing 100190, China

[a)]Author to whom correspondence should be addressed: le.fang@zoho.com

ABSTRACT

We solve analytically the period of a single triad interaction of homogeneous isotropic turbulence. Comparing with the traditional concept of the timescale of energy transfer, we found that this period is a timescale of energy exchange among the three wave vectors of a triad. Quantitatively, the timescale of energy exchange is usually longer if the equilibrium dissipation law is satisfied; however, when energy transfer is suppressed, the energy exchange becomes dominant. We extract the periods in typical numerical experiments of triad interactions and show that they are in good agreement with theoretical predictions. This picture implies that energy exchange corresponds to oscillation, while energy transfer corresponds to damping, and the damping rate is correlated with the oscillation. The present results of the timescale of energy transfer are expected to be applied in nonequilibrium turbulent flows.

I. INTRODUCTION

Turbulent flows typically feature chaos and spatiotemporal complexity, amongst other characteristics. From the energy point of view, in turbulent flows, the externally injected large-length-scale kinetic energy fluxes successively across intermediate spatial scales and ultimately dissipate at small scales. This whole process by which the kinetic energy can achieve a dynamic balance is known as the energy cascade. Kolmogorov first proposed the fundamental theory for the turbulent energy cascade (K41).[1] Based on the homogeneity assumptions at small scales, the $-5/3$ slope was obtained in the inertial range of the energy spectrum for a fully developed turbulent flow at a very high Reynolds number.[1] Kolmogorov's asymptotic results show that apart from the large-scale range, some statistical properties of turbulent flows should be universal, and in addition, they introduce scale-dependent characteristic times to quantify the energy cascade. In homogeneous isotropic turbulence, the only characteristic time is the eddy turn-over timescale (the typical timescale for an eddy to undergo a significant distortion), which can be obtained based on dimensional analysis and the equilibrium dissipation law.[1–3] In the inertial range, we can define the energy flux $\Pi(k)$ over a wavenumber k, and then, dimensional analysis can be written as

$$\Pi(k) = k^4 E(k)^2 \theta(k), \tag{1}$$

where $E(k)$ is the energy spectrum and $\theta(k)$ is the eddy turn-over timescale. According to K41, the energy spectrum obeys the $-5/3$ power law, namely, $E(k) = C_K \varepsilon^{2/3} k^{-5/3}$, with C_K the Kolmogorov constant and ε the rate of energy dissipation. In the current paper, we choose $C_K \approx 1.5$, a widely used constant.[4,5] Moreover, if the equilibrium dissipation law (a basic assumption of K41) is satisfied, the energy flux $\Pi(k)$ should be equal to the dissipation rate ε when k is in the inertial range. These relations finally yield

$$\theta(k) = C_K^{-2} \varepsilon^{-1/3} k^{-2/3}. \tag{2}$$

In homogeneous isotropic turbulence, this eddy turn-over timescale describes a universal property of energy transfer at wavenumber k.

On the other hand, it is commonly accepted that the energy transfer from large to small scales is due to nonlinear triad interactions of the Navier–Stokes equations between different wavenumbers;[6–8] thus, the eddy turn-over timescale is considered to be analogous to the characteristic timescale of nonlinear triad interactions.[9,10] Since a triad interaction can involve three different wavenumbers k, p, and q, taking the harmonic mean of the three eddy turn-over times is one way of estimating the characteristic timescale associated with triadic interactions, i.e.,

$$\theta_{kpq} = \left(\frac{\theta_k^{-1} + \theta_p^{-1} + \theta_q^{-1}}{3} \right)^{-1}. \tag{3}$$

This approximate timescale has been widely used in analytical turbulence closures to describe the "eddy damping."[9,11] According to Ref. 11, the concept of eddy damping is to replace the memory integral of the viscosity term of the equation of third-order cumulants; thus, we can regard this as a characteristic evolution time of the total energy of the triad, corresponding to the picture that energy transfer toward other wave vectors. Accordingly, we will call θ_{kpq} *the timescale of energy transfer*. Though nonlocal contribution always exists in triad interactions, it can be covered by other interactions as illustrated by the theoretical argument of Waleffe[8] and the numerical results of Zhou,[4] and ultimately, the energy cascade in the inertial range manifests itself as local interactions (namely, wave vectors in the triad are of similar length). If we only consider local triad interactions, the timescale of energy transfer is similar to the eddy turn-over timescale of any wave vector in the triad.

It follows directly from Eqs. (2) and (3) that the timescale of energy transfer is related to ε, which is connected with molecular viscosity. However, since global energy flux is not always balanced with dissipation, there must exist a timescale that is not related to molecular viscosity. A simple thought experiment is to imagine that we suddenly reduce (or increase) the molecular viscosity in a fully developed equilibrium turbulence, and then, ε immediately changes. However, the energy flux, which is related to nonlinear advection, will not change in a very short time, implying that the timescale should not change by Eq. (1). Also, the energy flux can be heavily suppressed and does not balance with dissipation.[12–14] It, then, follows that a new timescale, unrelated to dissipation, needs to be introduced, which can only be associated with the wavenumber k and the characteristic velocity $\mathcal{U}$, namely,

$$\mathcal{T} \propto k^{-1}\mathcal{U}^{-1}. \tag{4}$$

This dimension is formally the same as the Heisenberg time,[15,16] but the underlying pictures are different. According to Refs. 16 and 17, the Heisenberg time was introduced to explain the time delay of correlation functions, together with other time scales (see Refs. 18–20). Also, these time scales are combinations of dimensions rather than exact values.

In the present paper, we will derive a timescale with exact expressions, by starting from a single triad interaction without viscosity. We call this *the timescale of energy exchange*. Physically, this corresponds to the period of energy exchange among the three wave vectors and is not related to viscosity, as shown in Eq. (4). An intuitive picture on the time scales of "energy exchange" and "energy transfer" is that the former describes the oscillation of the energy at a single wave vector, while the latter describes the damping of amplitude of the energy.

The rest of this paper is organized as follows: In Sec. II, we derive the exact formula of the timescale of energy exchange, which is in the same order as (4). Specifically, in Sec. II C, we show that this timescale is usually longer than the timescale of energy transfer, indicating that in real turbulence with the equilibrium dissipation law, the timescale of energy exchange is not dominant. However, in some typical examples where energy transfer is suppressed in a short time, the timescale of energy exchange is dominant and can be clearly observed in numerical experiments as shown in Sec. III based on the direct numerical simulation (DNS). Finally, a conclusion is given in Sec. IV.

II. PERIOD OF A SINGLE TRIAD INTERACTION

Following Refs. 8, 21, and 22, we represent the velocity field of an incompressible fluid by using the helical decomposition. We transform the velocity field $\boldsymbol{v}(\boldsymbol{x})$ in physical space to $\boldsymbol{u}(\boldsymbol{k})$ in Fourier space with $\boldsymbol{k}$ the wave number vector. Being divergence-free due to incompressibility, $\boldsymbol{k}\cdot\boldsymbol{u}(\boldsymbol{k})=0$, each velocity component in Fourier space has only two degrees of freedom, and hence, two complex helical waves $\boldsymbol{h}^{\pm} = \hat{\boldsymbol{w}}\times\hat{\boldsymbol{k}} \pm \mathrm{i}\hat{\boldsymbol{w}}$ can form orthogonal bases, where $\mathrm{i}=\sqrt{-1}$, known as the imaginary unit. Here, the unit vector $\hat{\boldsymbol{w}}$ can be chosen as $\hat{\boldsymbol{w}} = \boldsymbol{z}\times\boldsymbol{k}/|\boldsymbol{z}\times\boldsymbol{k}|$ for an arbitrary vector $\boldsymbol{z}$. It, then, follows that

$$\boldsymbol{u}(\boldsymbol{k}) = u^{+}(\boldsymbol{k})\boldsymbol{h}^{+}(\boldsymbol{k}) + u^{-}(\boldsymbol{k})\boldsymbol{h}^{-}(\boldsymbol{k}). \tag{5}$$

Under this decomposition, the Navier–Stokes equations can be rewritten as

$$\left(\partial_t + \nu k^2\right)u^{s_k}(\boldsymbol{k}) = -\frac{1}{4}\sum_{\boldsymbol{k}+\boldsymbol{p}+\boldsymbol{q}=0}\sum_{s_p,s_q}(s_p p - s_q q) \times\left[\boldsymbol{h}^{s_p}\times\boldsymbol{h}^{s_q}\cdot\boldsymbol{h}^{s_k}\right]\bar{u}^{s_p}(\boldsymbol{p})\bar{u}^{s_q}(\boldsymbol{q}), \tag{6}$$

where ν is the kinematic viscosity, the overbar stands for complex conjugation, and the superscripts $s_k, s_p, s_q = +/-$ denote different helical modes. It is remarked that when s_k, s_p, s_q appear as variables in formulas, they are equal to ± 1.

The quadratic nature of the Navier–Stokes equations indicates that nonlinear triad interactions play an important role in homogeneous turbulence.[8] The triad interactions are defined by assuming that energy transfer only occurs among three wave numbers $(\boldsymbol{k},\boldsymbol{p},\boldsymbol{q})$ with specific helical modes (s_k, s_p, s_q). In the inviscid limit, this leads to a nonlinear system formed of three complex ordinary differential equations (ODEs) as follows:

$$\begin{aligned}
\dot{u}^{s_k}(\boldsymbol{k}) &= g(s_p p - s_q q)\bar{u}^{s_p}(\boldsymbol{p})\bar{u}^{s_q}(\boldsymbol{q}),\\
\dot{u}^{s_p}(\boldsymbol{p}) &= g(s_q q - s_k k)\bar{u}^{s_q}(\boldsymbol{q})\bar{u}^{s_k}(\boldsymbol{k}),\\
\dot{u}^{s_q}(\boldsymbol{q}) &= g(s_k k - s_p p)\bar{u}^{s_k}(\boldsymbol{k})\bar{u}^{s_p}(\boldsymbol{p}),
\end{aligned} \tag{7}$$

where the overdot denotes the time derivative and $g = -\frac{1}{4}[\boldsymbol{h}^{s_p}\times\boldsymbol{h}^{s_q}\times\boldsymbol{h}^{s_k}]$ is a prefactor. As shown in Ref. 8, these equations are formally similar to the Euler equations for the motion of a solid body around one of its points, which are defined in real space. Following a standard argument, it is easy to derive two first integrals (i.e., conserved physical quantities) from Eq. (7) as follows:

$$\begin{aligned}
|u^{s_k}|^2 + |u^{s_p}|^2 + |u^{s_q}|^2 &= \text{const.},\\
s_k k|u^{s_k}|^2 + s_p p|u^{s_p}|^2 + s_q q|u^{s_q}|^2 &= \text{const.},
\end{aligned} \tag{8}$$

corresponding to the conservation of energy and the conservation of helicity, respectively. It is noted that for complex unknowns, we can deduce differential equations of modulus and complex arguments for all velocity components (see Appendix A).

Equation (7) describes a single triad interaction, which assumes that energy only exchanges among three wave vectors and does not transfer to any wave vector outside. As pointed out in Ref. 23, usually a single triad interaction cannot correctly predict the long-term dynamics, but we will show in Sec. III that if energy transfer is suppressed in a short time, the energy exchange can be reproduced by direct numerical simulations (DNS).

In the following, we analytically investigate Eq. (7) for real u^{s_k}, u^{s_p}, u^{s_q}, and g and focus on the period of nonlinear energy transfer. Cases for the complex prefactor and unknowns have also been checked numerically in Appendix B. It is found that the periods for

real and complex cases have little difference, and at least, they are of the same order of magnitude (see also Ref. 24). As illustrated in Appendix C, in some situations, which correspond to the cases in Sec. III A, the periods for real and complex cases are exactly the same. Therefore, for the sake of simplicity, we will only focus on the real cases in the subsequent analyses.

A. Two of s_{kk}, s_{pp}, and s_{qq} being equal

It is obvious that if $s_k k = s_p p = s_q q$ holds, there is no energy transfer between different modes. When two of s_{kk}, s_{pp}, and s_{qq} are equal, without loss of generality, it suffices to consider $s_k k = s_p p > s_q q$ here. Then, the system (7) reduces to

$$\begin{aligned} \dot{u}^{s_k}(\boldsymbol{k}) &= g(s_p p - s_q q) u^{s_p}(\boldsymbol{p}) u^{s_q}(\boldsymbol{q}), \\ \dot{u}^{s_p}(\boldsymbol{p}) &= g(s_q q - s_k k) u^{s_q}(\boldsymbol{q}) u^{s_k}(\boldsymbol{k}), \\ \dot{u}^{s_q}(\boldsymbol{q}) &= 0, \end{aligned} \tag{9}$$

and we can rearrange equalities (8) as

$$\begin{aligned} |u^{s_p}|^2(\boldsymbol{p}) &= \frac{s_q q T - H}{s_q q - s_k k} - |u^{s_k}|^2(\boldsymbol{k}), \\ |u^{s_q}|^2(\boldsymbol{q}) &= \frac{s_k k T - H}{s_k k - s_q q}, \end{aligned} \tag{10}$$

where $T = |u^{s_k}|^2 + |u^{s_p}|^2 + |u^{s_q}|^2$ and $H = s_k k |u^{s_k}|^2 + s_p p |u^{s_p}|^2 + s_q q |u^{s_q}|^2$ are conserved energy and helicity, respectively. Solutions to this system are trigonometric functions, taking the form of

$$\begin{aligned} u^{s_k}(\boldsymbol{k}) &= \pm \sqrt{\frac{s_q q T - H}{s_q q - s_k k}} \sin\left(g \sqrt{(s_k k - s_q q)(s_k k T - H)} (t - t_0) \right), \\ u^{s_p}(\boldsymbol{p}) &= \pm \sqrt{\frac{s_q q T - H}{s_q q - s_k k}} \cos\left(g \sqrt{(s_k k - s_q q)(s_k k T - H)} (t - t_0) \right), \\ u^{s_q}(\boldsymbol{q}) &= \pm \sqrt{\frac{s_k k T - H}{s_k k - s_q q}}, \end{aligned} \tag{11}$$

where

$$t_0 = \mp \frac{1}{g \sqrt{(s_k k T - H)(s_k k - s_q q)}} \sin^{-1}\left(\sqrt{\frac{s_q q - s_k k}{s_q q T - H}} u_0^{s_k}(\boldsymbol{k}) \right),$$

with $u_0^{s_k}(\boldsymbol{k})$ the initial value of $u^{s_k}(\boldsymbol{k})$, and the sign of each equation is determined by the initial conditions. It follows directly from the solutions that the period of energy transfer is

$$\mathcal{T} = \frac{\pi}{g \sqrt{(s_k k - s_q q)(s_k k T - H)}}. \tag{12}$$

Note that $u^{s_k}(\boldsymbol{k})$ has twice the period of energy, which is defined as $(u^{s_k}(\boldsymbol{k}))^2$.

In Subsection II B, a similar formulation of the period of energy transfer will be obtained for the more general case, and we will elaborate on its physical interpretation.

B. None of s_{kk}, s_{pp}, and s_{qq} being equal

Without loss of generality, we assume $s_p p > s_k k > s_q q$. According to Eq. (8), $|u^{s_p}|^2(\boldsymbol{p})$ and $|u^{s_q}|^2(\boldsymbol{q})$ can be represented by $|u^{s_k}|^2(\boldsymbol{k})$ as

$$\begin{aligned} |u^{s_p}|^2(\boldsymbol{p}) &= \frac{s_q q - s_k k}{s_q q - s_p p} \left(\frac{s_q q T - H}{s_q q - s_k k} - |u^{s_k}|^2(\boldsymbol{k}) \right), \\ |u^{s_q}|^2(\boldsymbol{q}) &= \frac{s_p p - s_k k}{s_p p - s_q q} \left(\frac{s_p p T - H}{s_p p - s_k k} - |u^{s_k}|^2(\boldsymbol{k}) \right). \end{aligned} \tag{13}$$

Substituting (13) into (7), we can obtain, by employing the elliptic integration,

$$\int_{u_0^{s_k}}^{u^{s_k}(t)} \frac{du}{\sqrt{a^2 - u^2}\sqrt{b^2 - u^2}} = \pm g \sqrt{(s_k k - s_q q)(s_p p - s_k k)}\, t, \tag{14}$$

where $a^2 = \frac{s_q q T - H}{s_q q - s_k k}$ and $b^2 = \frac{s_p p T - H}{s_p p - s_k k}$. Note that the positivity of a^2 and b^2 can be demonstrated by substituting $T = |u^{s_k}|^2 + |u^{s_p}|^2 + |u^{s_q}|^2$ and $H = s_k k |u^{s_k}|^2 + s_p p |u^{s_p}|^2 + s_q q |u^{s_q}|^2$ into their definitions. Therefore, solutions to the triad interaction (7) can be expressed as the Jacobi elliptic functions. When $a^2 < b^2$, one obtains

$$\begin{aligned} u^{s_k}(\boldsymbol{k}) &= \pm \sqrt{\frac{s_q q T - H}{s_q q - s_k k}} \operatorname{sn}\left(g \sqrt{(s_k k - s_q q)(s_p p T - H)} (t - t_0) \right), \\ u^{s_p}(\boldsymbol{p}) &= \pm \sqrt{\frac{s_q q T - H}{s_q q - s_p p}} \operatorname{cn}\left(g \sqrt{(s_k k - s_q q)(s_p p T - H)} (t - t_0) \right), \\ u^{s_q}(\boldsymbol{q}) &= \pm \sqrt{\frac{s_p p T - H}{s_p p - s_q q}} \operatorname{dn}\left(g \sqrt{(s_k k - s_q q)(s_p p T - H)} (t - t_0) \right), \end{aligned} \tag{15}$$

where

$$t_0 = \mp \frac{1}{g \sqrt{(s_p p T - H)(s_k k - s_q q)}} \operatorname{sn}^{-1}\left(\sqrt{\frac{s_q q - s_k k}{s_q q T - H}} u_0^{s_k}(\boldsymbol{k}) \right),$$

with $u_0^{s_k}(\boldsymbol{k})$ the initial value of $u^{s_k}(\boldsymbol{k})$, and the sign of each equation is determined by the initial conditions.

According to the properties of elliptic functions: $u^{s_k}(\boldsymbol{k})$ and $u^{s_p}(\boldsymbol{p})$ have a period of $\frac{4K}{g\sqrt{(s_k k - s_q q)(s_p p T - H)}}$, while their signs change with time symmetrically; $u^{s_q}(\boldsymbol{q})$ has a period of $\frac{2K}{g\sqrt{(s_k k - s_q q)(s_p p T - H)}}$ with a fixed sign. Here, K is the complete elliptic integral defined as

$$K = \int_0^1 \frac{du}{\sqrt{(1 - u^2)(1 - \alpha^2 u^2)}},$$

with $\alpha = |a/b| < 1$. Thus, the energy transfer period of the triad system reads

$$\mathcal{T} = \frac{2K}{g \sqrt{(s_k k - s_q q)(s_p p T - H)}}. \tag{16}$$

It is clear that the theoretical predictions of the period, Eqs. (16) and (12), are formally similar. As a special case, solutions are no longer periodic functions for the case of $a^2 = b^2$, and the reader is referred to Appendix D for more details. We remark that the solution (15) has already been noticed by Bustamante and Kartashova[24,25] by using the Hamiltonian formulation, but the details were not represented. Moreover, the derivations presented here allow further discussions on the physical interpretations.

In the present paper, the exact formulas of the solutions, i.e., Eqs. (16) and (12), are not of interest. Instead, we are rather interested in the underlying timescale $\mathcal{T}$ in these solutions. The physical interpretations are explained as follows. Considering the same shape of triad with different moduli of wave vectors, i.e., enlarging k, p, and q proportionally, from Eqs. (16) and (12), we have $\mathcal{T} \propto k^{-1}$. On the other hand, enlarging $u^{s_k}, u^{s_p}, u^{s_q}$ proportionally gives $\mathcal{T} \propto \mathcal{U}^{-1}$, where $\mathcal{U}$ is the characteristic velocity scale. It, then, follows directly from the scaling (4) that the newly defined timescale is a "purely advective" timescale and unrelated to viscosity. We will show in Subsection II C that the new timescale has completely different physics in comparison with the timescale of energy transfer.

C. Quantitative comparison with the timescale of energy transfer

The concept of the timescale of energy exchange is completely different from the timescale of energy transfer θ_{kpq}. According to our derivations in Subsections II A and II B, when three wave vectors exchange energy, we do not consider any energy transfer to other wave vectors, and the total energy of $(\boldsymbol{k}, \boldsymbol{p}, \boldsymbol{q})$ is conserved. In the following, we will first compare the magnitudes of two time scales, then analyze the difference in physics between them, and illustrate the reasonableness of the timescale of energy exchange.

According to Eqs. (16) and (12), the timescale of energy exchange depends not only on k, p, and q but also on the helical modes s_k, s_p, s_q; therefore, we denote by $\mathcal{T}_{k,p,q}(s_k, s_p, s_q)$ the timescale of energy change. By contrast, the timescale of energy transfer θ_{kpq} does not depend on helical modes. Recalling the traditional expression of θ_{kpq}, i.e., Eq. (3), the timescale of energy transfer appears as a harmonic mean of the time scales of all wave vectors. The underlying intuition is that the fastest-evoluting mode is dominant in the global evolution of the triad. It is similar for the timescale of energy exchange since the fastest-developing triad among different combinations of helical modes should be dominant for fixed (k, p, q). Consequently, following Ref. 9 and using the harmonic mean, we define a global timescale at (k, p, q) by considering all helical modes,

$$\theta^c_{kpq} = \left(\frac{1}{8} \sum_{s_k, s_p, s_q} \mathcal{T}_{k,p,q}(s_k, s_p, s_q)^{-1} \right)^{-1}. \tag{17}$$

The quantitative comparison between θ^c_{kpc} and θ_{kpq} is performed by assuming that (k, p, q) are located in the inertial range with the $-5/3$ energy spectrum $E(k)$. From Eq. (5), the modal kinetic energy can be given by $\frac{1}{2}\boldsymbol{u}(\boldsymbol{k})\bar{\boldsymbol{u}}(\boldsymbol{k}) = u^+(\boldsymbol{k})\bar{u}^+(\boldsymbol{k}) + u^-(\boldsymbol{k})\bar{u}^-(\boldsymbol{k})$. Another parameter $\alpha_{s_k} = (u^{s_k}(\boldsymbol{k})\bar{u}^{s_k}(\boldsymbol{k}))/(\frac{1}{2}\boldsymbol{u}(\boldsymbol{k})\bar{\boldsymbol{u}}(\boldsymbol{k}))$ is introduced to account for the ratio between the helical mode s_k and the total energy of $\boldsymbol{k}$. For isotropic turbulence, the energy of a shell with a radius k in Fourier space can be written as

$$(\Delta k)E(k) = 2\pi \frac{k^2}{(\Delta k)^2} \langle \boldsymbol{u}(\boldsymbol{k})\bar{\boldsymbol{u}}(\boldsymbol{k}) \rangle,$$

where Δk denotes the mesh size and $\langle \cdot \rangle$ is an ensemble average operator (see Ref. 26). This equation connects the energy in discrete and continuous spaces. The total energy T and the total helicity H in helical modes (s_k, s_p, s_q) can be, thereby, calculated as

$$\begin{aligned} T &= \alpha_{s_k} \frac{E(k)}{4\pi k^2} (\Delta k)^3 + \alpha_{s_p} \frac{E(p)}{4\pi p^2} (\Delta k)^3 + \alpha_{s_q} \frac{E(q)}{4\pi q^2} (\Delta k)^3 \\ &= \frac{C_K \varepsilon^{\frac{2}{3}} (\Delta k)^3}{4\pi} \left(\alpha_{s_k} k^{-\frac{11}{3}} + \alpha_{s_p} p^{-\frac{11}{3}} + \alpha_{s_q} q^{-\frac{11}{3}} \right), \\ H &= s_k \alpha_{s_k} \frac{E(k)}{4\pi k} (\Delta k)^3 + s_p \alpha_{s_p} \frac{E(p)}{4\pi p} (\Delta k)^3 + s_q \alpha_{s_q} \frac{E(q)}{4\pi q} (\Delta k)^3 \\ &= \frac{C_K \varepsilon^{\frac{2}{3}} (\Delta k)^3}{4\pi} \left(\alpha_{s_k} k^{-\frac{8}{3}} + \alpha_{s_p} p^{-\frac{8}{3}} + \alpha_{s_q} q^{-\frac{8}{3}} \right). \end{aligned} \tag{18}$$

Since the triad interaction is defined at discrete wave vectors whose extremities follow the nodes of a regular grid of mesh, we denote $k = m\Delta k$, $p = n\Delta k$, and $q = l\Delta k$ with $m^2, n^2, l^2 \in \mathbb{N}$. The discretized eddy-damping time can, then, be written as

$$\theta_{mnl} = \left(\frac{\theta_m^{-1} + \theta_n^{-1} + \theta_l^{-1}}{3} \right)^{-1},$$

where $\theta_m = (\frac{1}{2})^{\frac{1}{3}} \varepsilon^{-\frac{1}{3}} m^{-\frac{2}{3}} (\Delta k)^{-\frac{2}{3}}$.[9] Similarly, we can obtain the formula for θ^c_{mnl} by substituting Eq. (18) into energy transfer periods. Subsequently, we can calculate the ratio of these two time scales $R_{mnl} = \theta_{mnl}/\theta^c_{mnl}$, which does not depend on Δk or ε.

It is found that $R_{mnl} \ll 1$ in most cases, indicating that the timescale of energy exchange is usually much longer than the eddy-damping timescale. For example, if we select $\alpha_+ = \alpha_- = 0.5$, then $R_{\{1,1,\sqrt{2}\}} = 0.019\,8$. We can obtain $R_{mnl} \gtrsim 1$ only when two legs of the triangle are much longer than the third one, for example, $R_{\{1,100000,100000\}} = 1.074\,1$. This fact means that in real turbulence, the energy transfer from a triad to other wave vectors is usually much faster than the energy exchange. This explains why in traditional turbulence closures we only need the eddy-damping timescale and never consider the timescale of energy exchange. However, we will show in Sec. III that in particular cases, when transfer is not balanced with dissipation, the energy exchange among the three wave vectors can be important, and the period is in good agreement with the theoretical prediction. Specifically, we will consider the case that a triad transfers energy to outside very slowly.

III. NUMERICAL RESULTS

As discussed above, in real turbulence, a triad is more likely to transfer energy to outside, rather than exchange energy among the three wave vectors, because the timescale of energy exchange is usually much smaller than the timescale of energy transfer. However, we should remark that the timescale of energy transfer is usually used to characterize turbulent flows where transfer and dissipation are equilibrium. There also exist turbulent flows out of equilibrium. To give an extreme example, energy transfer can be fully eliminated if a parallel relation is satisfied in a single-scale flow,[14] but unfortunately, triad interactions are also eliminated in this situation. To overcome the difficulty, here we only inject initial energy into several typical wave vectors, and it can be proved that the initial zero-energy wave vectors will receive energy in the magnitude of $O(t^{2n})$, where $n \geq 1$ is a positive integer representing the distance to energy-containing wave vectors.[13] This estimate implies that these zero-energy modes will not change significantly in a short time, or equivalently, the energy-containing modes do not transfer energy to others in a short time. Under such circumstances, we are able to focus on the energy exchange in a triad and investigate the time scales.

Direct numerical simulations for the full Navier–Stokes equations are performed by using a standard pseudo-spectral solver and a fourth-order Runge–Kutta time integration scheme, with a semi-implicit treatment of the viscous term.[27] The computational domain is a periodic box in three dimensions with a staggered grid of size 128^3, corresponding to maximum wavenumber $k_{\max} = 64$ in Fourier space. A hyperviscosity term in the form of $\nabla^4 \boldsymbol{v}$ is introduced to prevent the truncation accumulation at high wavenumbers, while it hardly affects lower wavenumbers.[28]

In Subsections III A and III B, we will show two types of examples, which correspond to the local and nonlocal triad interactions, respectively. By statistical analysis, these two types of triad interactions were found to contribute to the local energy transfer via different mechanisms, respectively.[29,30] We will show that the timescale of energy exchange exists in both types of triad interactions.

A. Local triad interactions

The initial field here is generated by injecting energy into an 18-wave set, as shown in Fig. 1. We have tested different initial fields and selected two typical cases described in Table I, which can result in the simplest and purest triad interactions (other cases are mixtures of these two).

As explained above, a striking feature of this initial field is that although triad interactions always exist, the mean energy on a sphere of wave vectors remains constant in a short time by neglecting the viscosity, namely,

$$\dot{e}(k)|_{t=0} = 0\,, \quad \forall k = \sqrt{\kappa}\,, \quad \kappa \in \mathbb{N}_+, \tag{19}$$

where $e(k)$ is defined as

$$e(k) := \frac{1}{N_k} \sum_{|\boldsymbol{k}|=k} \left(u^+(\boldsymbol{k})^2 + u^-(\boldsymbol{k})^2\right), \tag{20}$$

with N_k the number of waves satisfying $|\boldsymbol{k}| = k$. We omit the detailed proof, and the interested reader is referred to Ref. 13.

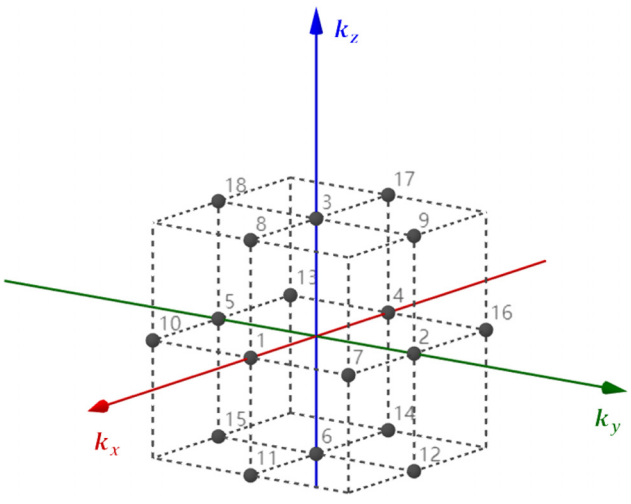

FIG. 1. Sketch of the initial 18-wave set that contains energy. Numbers are identifiers of different waves.

TABLE I. Initial velocities in different numerical cases.

Case	Wave identifiers[a]	Wavenumber	Helical mode	Initial value
A	1–6	1	u^+	1.0
			u^-	0.0
	7–18	$\sqrt{2}$	u^+	0.5
			u^-	0.0
B	1–6	1	u^+	1.0
			u^-	0.0
	7–18	$\sqrt{2}$	u^+	0.0
			u^-	0.5

[a]Corresponding to the numbers in Fig. 1.

We remark that the definition of $e(k)$ differs from the traditional definition of the energy spectrum, in which energy is averaged on a continuous sphere. We call $e(k)$ the "discrete energy spectrum" since it is an average over discrete Fourier modes. A difference is that approximating the continuous energy spectrum by using discrete points will lead to integration errors.[31] Moreover, from the present definition, some integer wavenumbers of k^2 do not contain energy, such as $k^2 = 7, 15$, and 23, since they cannot be expressed as a summation of three complete square numbers. However, as will be shown in the subsequent parts, the general envelope of $e(k)$ is similar to the traditional energy spectrum.

The time evolution of total energy is shown in Fig. 2. In the early stages, both cases approximately conserve energy since most energies are stored at small wavenumbers, which are hardly influenced by the hyperviscosity $\nabla^4 \boldsymbol{v}$. In the long time dynamics, both cases decay via a $t^{-2.6}$ scaling, with the exponent related to the form of hyperviscosity. An obvious difference between these two cases is that case B decays earlier than case A ($t \sim 2$ vs $t \sim 3$). This indicates that the same initial energy spectra can lead to different energy evolutions. We show the discrete energy spectra $e(k)$ in Fig. 3. At $t = 0$, there are only two wavenumbers containing energy, as designed in Table I. Energy is, then, transferred to higher wavenumbers via triad interactions, dissipates at the highest wavenumbers due to hyperviscosity, and finally features a $-5/3$ inertial range in spectra for both cases.

Figure 4 shows the time evolution of $e(k)$ for the first three wavenumbers. In general, $e(1)$ and $e(\sqrt{2})$ decay since energy is transferred to higher wavenumbers; $e(\sqrt{3})$ increases while receiving energy from smaller wavenumbers, and then decays by transferring energy to higher wavenumbers. The long-term decay of $e(1)$ satisfies the $t^{-2.6}$ law of total energy, illustrating that $e(1)$ is the dominant part of total energy; the short-term increase in $e(\sqrt{3})$ satisfies the t^2 law, corresponding to the scaling of small-scale response.[13]

The most striking phenomenon is that the discrete energy of case B oscillates much faster and stronger than that of case A, in particular for $e(1)$ and $e(\sqrt{2})$. This fluctuation, obviously, is quasiperiodic and should correspond to a specific timescale. The difference in parameters between cases A and B implies that this timescale should be related to the distribution of energy in helical modes u^+ and u^-, as predicted by the timescale of energy exchange. In the following, we will extract this period and compare it with the theoretical predictions in Sec. II.

In order to extract the period of fluctuation of $e(1)$ in case B, we decompose the signal by using the method of Prony analysis.[32,33] The

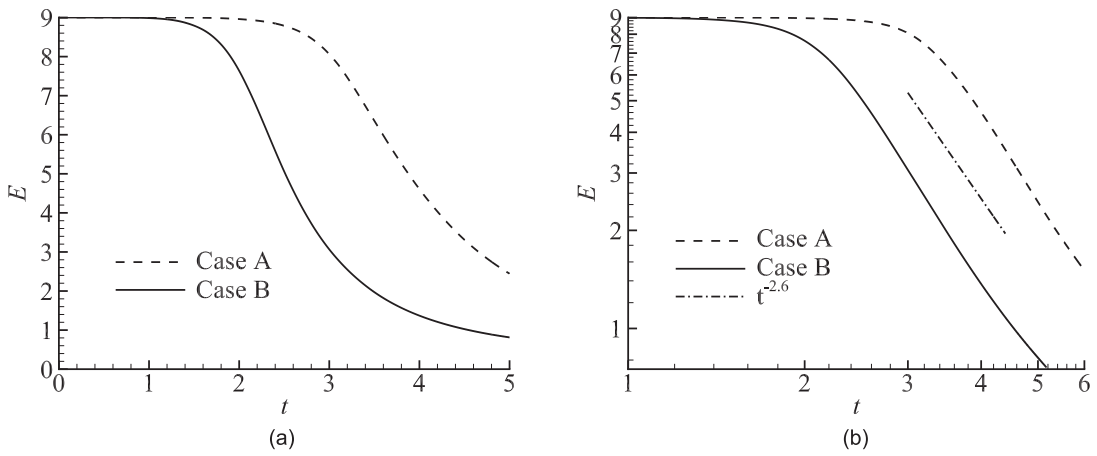

FIG. 2. Time evolution of the total energy: (a) normal view and (b) log–log view.

choice of Prony analysis, instead of other methods such as Fourier decomposition, is due to its capacity on those signals that vibrate and decay simultaneously. In Prony's method, an input signal $S(t)$ is represented by a sum of complex exponentials as $S(t) = \sum_{n=1}^{N} A_n e^{-ik_n t}$, where N is the maximum mode number with a numerical truncation and A_n and k_n are complex numbers standing for both modal amplitude and modal frequency, respectively. Note that the real part of k_n indicates the frequency of the n-th wave component. The dominant mode of the input signal can be defined as the mode with the largest amplitude $|A_n|$. After applying Prony's method to the signal with t from 0 to 4.25 and $N = 1700$, the period of the dominant mode of $e(1)$ is $\mathcal{T}_{\text{numerical}} = 1.912\,5$. For a robustness test, the original signal can be well reconstructed from summing the first 15 modal terms (see Appendix E for the details).

The theoretical prediction for the timescale of energy exchange can be obtained by substituting initial conditions of case B to Eqs. (16) and (12). For the first class modes in case B (namely, the length of wave vectors is equal to 1), at the initial moment, there are only five types of triad interactions according to elements of the ensemble $\{s_k k, s_p p, s_q q\} = \{1, 1, -\sqrt{2}\}, \{1, 1, \sqrt{2}\}, \{1, -1, -\sqrt{2}\}, \{1, -\sqrt{2}, \sqrt{3}\}$, and $\{1, -\sqrt{2}, -\sqrt{3}\}$. With the initial velocities shown in Table I, the period of energy transfer of each triad interaction can be calculated, yielding $\mathcal{T}_{\{1,1,-\sqrt{2}\}} = 12.566$, $\mathcal{T}_{\{1,1,\sqrt{2}\}} = +\infty$, $\mathcal{T}_{\{1,-1,-\sqrt{2}\}} = 2.8975$, $\mathcal{T}_{\{1,-\sqrt{2},\sqrt{3}\}} = 5.0497$, and $\mathcal{T}_{\{1,-\sqrt{2},-\sqrt{3}\}} = 1.9602$, respectively. The comparison between analytical and numerical results indicates that the smallest analytical period $\mathcal{T}_{\{1,-\sqrt{2},-\sqrt{3}\}} = 1.9602$ and the numerical value $\mathcal{T}_{\text{numerical}} = 1.9125$ are of the same order in magnitude with a very small relative difference,

$$e_r = \frac{\mathcal{T}_{\{1,-\sqrt{2},-\sqrt{3}\}} - \mathcal{T}_{\text{numerical}}}{\mathcal{T}_{\{1,-\sqrt{2},-\sqrt{3}\}}} = 2.43\%.$$

Here, the smallest period corresponds to the fastest energy evolution for wavenumber 1, which should be the most evident in short time. Since all triad interactions are coupled, this fastest energy evolution

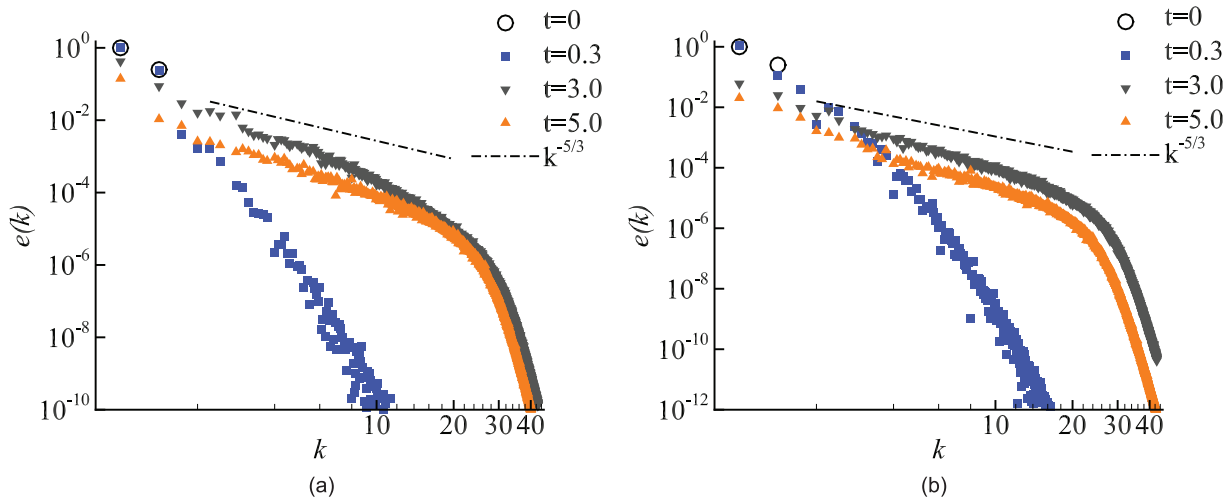

FIG. 3. Discrete energy spectra at different times: (a) case A and (b) case B.

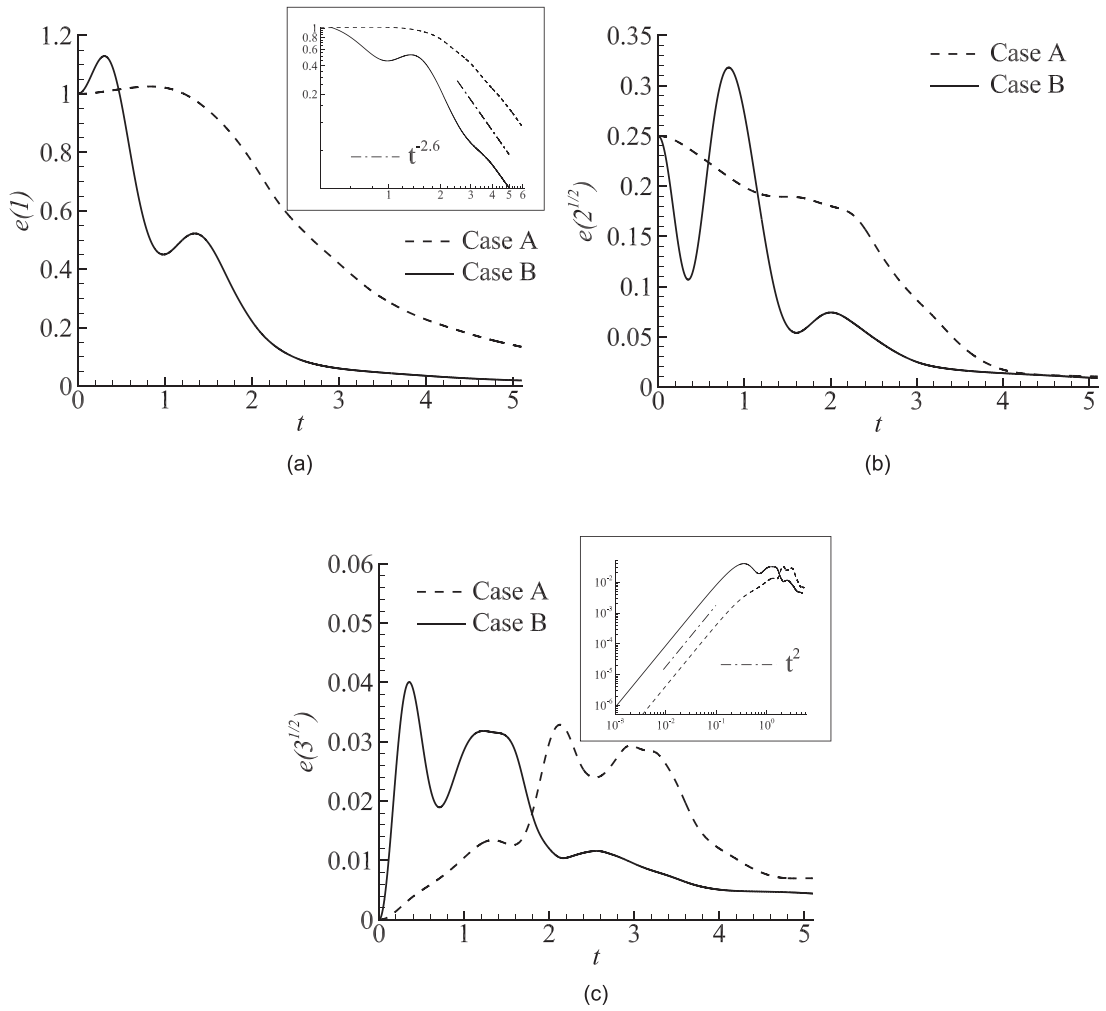

FIG. 4. Evolution of discrete averaged energy $e(k)$ for different wavenumbers: (a) $k=1$ with a subfigure log-log view focusing on long-term evolution, (b) $k=\sqrt{2}$, and (c) $k=\sqrt{3}$ with a subfigure log-log view focusing on short-term evolution.

will change the energy of wavenumber 1 in short time and then change all other longer periods accordingly. Therefore, it is not easy to observe longer periods in the present case. In brief, the oscillation of energy in a short time corresponds to the energy exchange in triad interactions, and the period of oscillation can be well predicted by the exact time-scale of energy exchange.

In addition, the theoretical timescale of energy exchange for case A can also be obtained by the same way. For the first-class modes in case A, at the initial moment, there are another five types of triad interactions according to elements of the ensemble $\{s_k k, s_p p, s_q q\} = \{1, 1, -\sqrt{2}\}$, $\{1, 1, \sqrt{2}\}$, $\{1, -1, \sqrt{2}\}$, $\{1, \sqrt{2}, \sqrt{3}\}$, and $\{1, \sqrt{2}, -\sqrt{3}\}$. With the initial conditions of case A, the period of energy transfer of each triad interaction can be calculated, yielding $\mathcal{T}_{\{1,1,\sqrt{2}\}} = 12.566$, $\mathcal{T}_{\{1,1,-\sqrt{2}\}} = +\infty$, $\mathcal{T}_{\{1,-1,\sqrt{2}\}} = 8.437\,1$, $\mathcal{T}_{\{1,\sqrt{2},\sqrt{3}\}} = 4.644\,5$, and $\mathcal{T}_{\{1,\sqrt{2},-\sqrt{3}\}} = 18.565$, respectively. Quantitatively, the global eddy turn-over time, defined as $T_{\text{to}} := \sqrt{3/2}(E/\epsilon)$, is approximately estimated as $T_{\text{to}}(\mathcal{T}_{\{1,\sqrt{2},-\sqrt{3}\}}/2) = 7.11$, the same order as $\mathcal{T}_{\{1,\sqrt{2},-\sqrt{3}\}} = 4.644\,5$. This indicates that the energy transfer effect is fast; thus, we cannot observe an oscillation of $e(1)$ for case A in Fig. 4(a). By contrast, for case B, the smallest period $\mathcal{T}_{\{1,-\sqrt{2},-\sqrt{3}\}} = 1.960\,2$ corresponds to a very large eddy turn-over time $T_{\text{to}}(\mathcal{T}_{\{1,-\sqrt{2},-\sqrt{3}\}}/2) = 110.07$, indicating that the energy transfer is slow, and thus, we can clearly observe the energy exchange effect.

B. Nonlocal triad interactions

In this subsection, we perform another DNS case corresponding to nonlocal triad interactions, where one leg in the triangle is short and the other two legs are long.

The numerical experiment is conducted in a periodic box with a grid of 64^3, corresponding to the maximum wavenumber $k_{\max} = 32$ in Fourier space. Initially, energy is only injected into the wave vectors

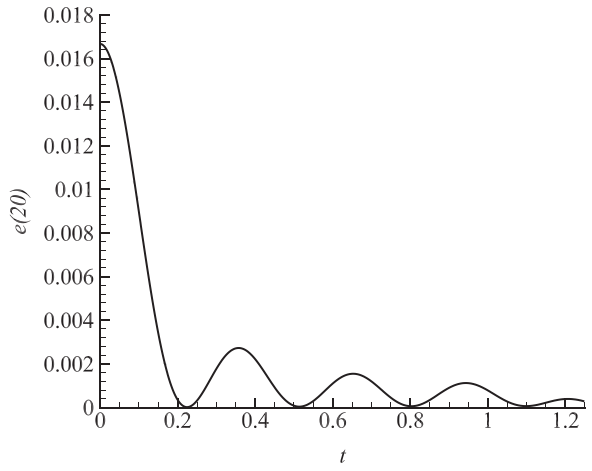

FIG. 5. Evolution of discrete averaged energy $e(20)$.

$u^+(0,0,1) = \bar{u}^+(0,0,-1) = 1$ and $u^-(20,0,0) = \bar{u}^-(-20,0,0) = 0.5$, while all other helical components are set to 0. The short time evolution of $e(20)$ is shown in Fig. 5.

Using the Prony analysis mentioned in Sec. III, $e(20)$ is reconstructed by 8 modal terms whose detailed information is shown in Appendix E, and the numerical result of period of fluctuation reads $\mathcal{T}_{\text{numerical}} = 0.567\,5$. Analytical predictions can be obtained by substituting initial conditions to Eq. (16), which turn out to be $\mathcal{T}_{\{1,-20,\sqrt{401}\}} = 24.352$ and $\mathcal{T}_{\{1,-20,-\sqrt{401}\}} = 0.586\,0$. The relative difference between the numerical value and the smallest analytical period is

$$e_r = \frac{\mathcal{T}_{\{1,20,-\sqrt{401}\}} - \mathcal{T}_{\text{numerical}}}{\mathcal{T}_{\{1,20,-\sqrt{401}\}}} = 3.16\%.$$

This very small difference indicates that the exact timescale of energy exchange is also well captured in nonlocal triad interactions.

IV. CONCLUSIONS

In this paper, we solve analytically the period of a single triad interaction. This period is regarded as the timescale of energy exchange. Specifically, it does not relate to viscosity, differing from the traditional concept of timescale of energy transfer. Quantitatively, the timescale of energy exchange is usually longer if the equilibrium dissipation law is satisfied. However, when energy transfer is suppressed, the energy exchange becomes dominant and can be clearly observed in numerical calculations. Good agreement between numerical results and theoretical predictions is achieved, and the relative differences are shown to be less than 4% for both local and nonlocal tested cases.

Formally, the timescale of energy exchange is derived under the helical decomposition, which implies that different combinations of helical modes can lead to different time scales, even if the total energy remains the same. In another word, the timescale of energy exchange involves new physics for the velocity phase [see Eq. (A3) for the formula], which is not considered in the timescale of energy transfer, i.e., Eqs. (1) and (2). In fact, the velocity phase has been illustrated to be one of the key factors in the nonequilibrium turbulent flows, in which transfer is no longer balances with dissipation.[3,12,13,34–36] As an example, Ref. 12 reverses all velocities, leading to a delay of decay. We, therefore, expect to apply the timescale of energy exchange in these flows to reveal more underlying physics in future studies.

ACKNOWLEDGMENTS

The authors are grateful to Haitao Xu, Shiyi Chen, Guowei He, Zixuan Yang, Ying Zhu, Xiaodong Jing, Xiaofeng Sun, and Emmanuel Riboulet-Deyris for very helpful discussions and to Yang Meng and Chuhan Wang for the scientific input. T.W. and L. F. were supported by the National Natural Science Foundation of China (Grant Nos. 11572025, 11772032, and 51420105008), and Z. W. was supported by the Strategic Priority Research Program of the Chinese Academy of Sciences (Grant No. XDB22040203).

APPENDIX A: EQUATIONS OF COMPLEX ARGUMENT IN TRIAD INTERACTIONS

In general cases, the prefactor g is a complex constant for each individual triad interaction, and the velocity modes are complex as well. We can express the helical modes and g by introducing the phases as follows:

$$\begin{aligned} u^{s_k}(\boldsymbol{k},t) &= |u^{s_k}|(\boldsymbol{k},t)e^{\mathrm{i}\theta_{s_k}(\boldsymbol{k},t)}, \\ u^{s_p}(\boldsymbol{p},t) &= |u^{s_p}|(\boldsymbol{p},t)e^{\mathrm{i}\theta_{s_p}(\boldsymbol{p},t)}, \\ u^{s_q}(\boldsymbol{q},t) &= |u^{s_q}|(\boldsymbol{q},t)e^{\mathrm{i}\theta_{s_q}(\boldsymbol{q},t)}, \\ g &= |g|e^{\mathrm{i}\theta_g}, \end{aligned} \tag{A1}$$

where $|u^{s_k}|$, $|u^{s_p}|$, $|u^{s_q}|$, $|g|$ are moduli and θ_{s_k}, θ_{s_p}, θ_{s_q}, and θ_g are phases. Substituting (A1) into (7), one obtains

$$\begin{aligned} &\frac{\partial|u^{s_k}|(\boldsymbol{k},t)}{\partial t}e^{\mathrm{i}\theta_{s_k}(\boldsymbol{k},t)} + \mathrm{i}|u^{s_k}|(\boldsymbol{k},t)\frac{\partial\theta_{s_k}(\boldsymbol{k},t)}{\partial t}e^{\mathrm{i}\theta_{s_k}(\boldsymbol{k},t)} \\ &= (s_p p - s_q q)g|u^{s_p}|(\boldsymbol{p},t)|u^{s_q}|(\boldsymbol{q},t)e^{-\mathrm{i}(\theta_{s_p}(\boldsymbol{p},t)+\theta_{s_q}(\boldsymbol{q},t))}. \end{aligned} \tag{A2}$$

The real and imaginary parts on both sides should be, respectively, equal; hence,

$$\begin{aligned} \frac{\partial|u^{s_k}|(\boldsymbol{k},t)}{\partial t} &= (s_p p - s_q q)|g||u^{s_p}|(\boldsymbol{p},t)|u^{s_q}|(\boldsymbol{q},t) \\ &\quad\cdot\cos(\theta_g - \theta_{s_k}(\boldsymbol{k},t) - \theta_{s_p}(\boldsymbol{p},t) - \theta_{s_q}(\boldsymbol{q},t)), \\ |u^{s_k}|(\boldsymbol{k},t)\frac{\partial\theta_{s_k}(\boldsymbol{k},t)}{\partial t} &= (s_p p - s_q q)|g||u^{s_p}|(\boldsymbol{p},t)|u^{s_q}|(\boldsymbol{q},t) \\ &\quad\cdot\sin(\theta_g - \theta_{s_k}(\boldsymbol{k},t) - \theta_{s_p}(\boldsymbol{p},t) - \theta_{s_q}(\boldsymbol{q},t)). \end{aligned} \tag{A3}$$

It is remarked that this type of phase equation is important for investigations of the one-dimensional Burgers equation.[37,38] We, then, expect that these new equations will inspire future studies on three-dimensional Navier–Stokes flows.

APPENDIX B: COMPARISON OF PERIODS OF TRIAD INTERACTIONS IN THE COMPLEX AND REAL FIELDS

In the complex field, Eq. (7) does not have an explicit solution; thus, periods of triad interactions cannot be obtained analytically. However, we can check the ratio of periods for complex and real

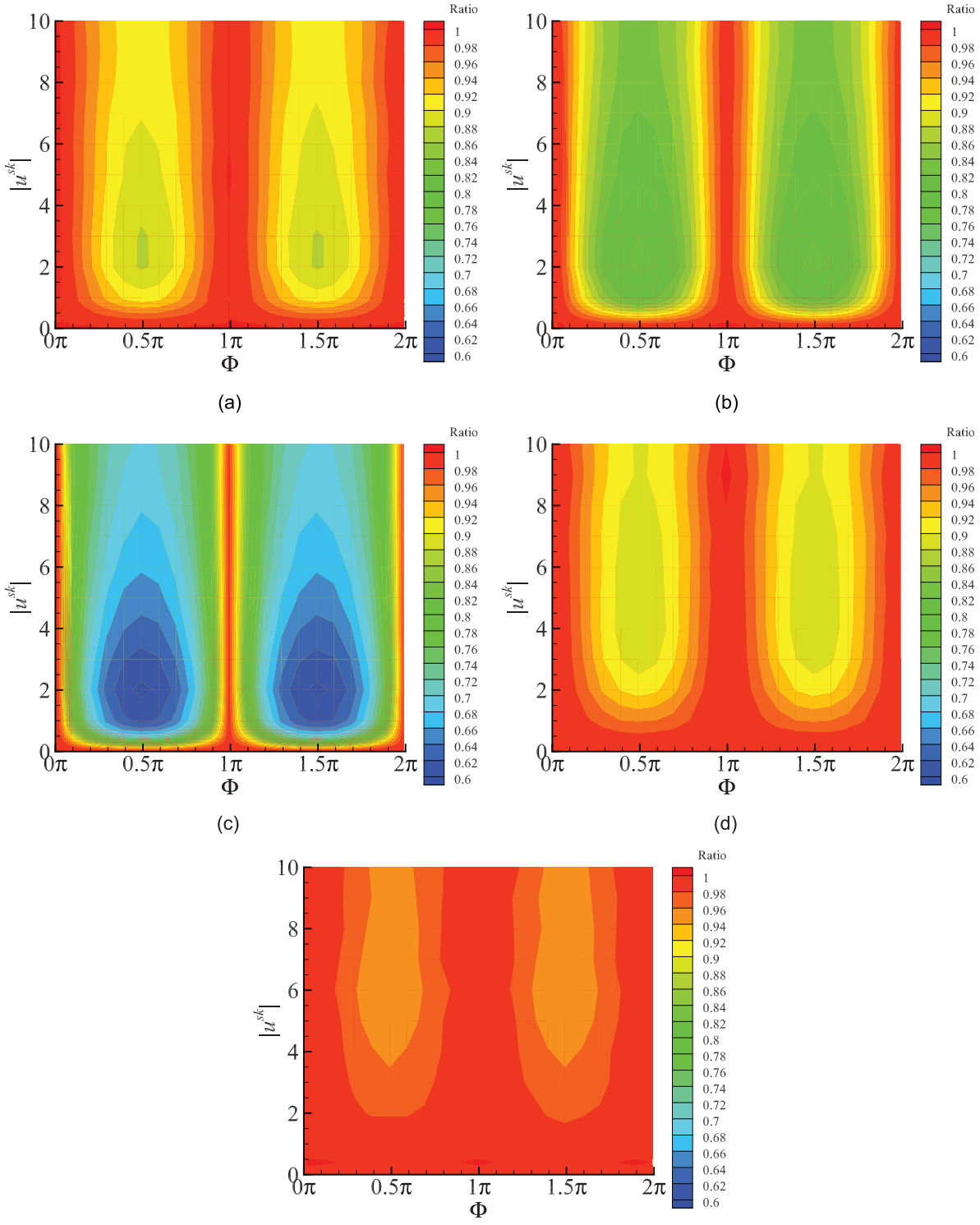

FIG. 6. Period ratio R of the triad interaction $(s_k k, s_p p, s_q q) = (1, 10.5, -10)$ with $|u^{s_q}|(t=0) = 1$, $\Phi(t=0)$ varies from 0 to 2π and $|u^{s_k}|(t=0)$ varies from 0 to 10. (a) $|u^{s_p}|(t=0) = 0.6$, (b) $|u^{s_p}|(t=0) = 0.8$; (c) $|u^{s_p}|(t=0) = 1$, (d) $|u^{s_p}|(t=0) = 2$, and (e) $|u^{s_p}|(t=0) = 3$.

cases numerically. This ratio can be defined as $R = \mathcal{T}_{complex}/\mathcal{T}_{real}$, where $\mathcal{T}_{real}$ is the energy transfer period of a triad system in the real field and $\mathcal{T}_{complex}$ denotes the period of the same triad interaction $(s_k k, s_p p, s_q q)$ with the complex prefactor and unknowns. In this section, we take $(s_k k, s_p p, s_q q) = (1, 10.5, -10)$ as an example to analyze the values of R under different initial conditions.

From the equations of complex argument and modulus [Eq. (A3)], it is observed that the "triad phase" $\Phi(\boldsymbol{k}, \boldsymbol{p}, \boldsymbol{q}, t) = \theta_g - \theta_{s_k}(\boldsymbol{k}, t) - \theta_{s_p}(\boldsymbol{p}, t) - \theta_{s_q}(\boldsymbol{q}, t)$ can lead to the variation of the timescale. Hence, the initial value of Φ has an impact on the period ratio R. Moreover, enlarging the moduli $|u^{s_k}|$, $|u^{s_p}|$, $|u^{s_q}|$ proportionally implies that $\mathcal{T} \propto \mathcal{U}^{-1}$, where $\mathcal{T}$ is the period of the triad interaction and $\mathcal{U}$ is the characteristic velocity scale. This statement holds for both real and complex fields according to Eq. (A3), and as a result, enlarging $|u^{s_k}|$, $|u^{s_p}|$, $|u^{s_q}|$ proportionally has no influence on the period ratio R. Without loss of generality, we fix $|u^{s_q}| = 1$ at the initial moment. The evolution of R with different initial values of $|u^{s_k}|$, $|u^{s_p}|$ and Φ is shown in Fig. 6. It is clear that the value of R is greater than 0.8 under most initial conditions. This numerical experiment indicates that the periods for real and complex cases are in the same order of magnitude.

APPENDIX C: PERIODS OF TRIAD INTERACTIONS AMONG COMPLEX MODES

If the prefactor g is a complex number, usually the period of energy exchange cannot be exactly the same as that in real cases. However, at least we can show that, for the five types of triad interactions mentioned in Sec. III A, i.e., $\{s_k k, s_p p, s_q q\} = \{1, 1, -\sqrt{2}\}$, $\{1, 1, \sqrt{2}\}$, $\{1, -1, -\sqrt{2}\}$, $\{1, -\sqrt{2}, \sqrt{3}\}$, and $\{1, -\sqrt{2}, -\sqrt{3}\}$, particular solutions can be obtained with initial conditions listed in case B of Table I. The periods of energy exchange for complex modes are the same as those for the real modes. This statement is proved in detail below.

(1) For the triad interaction $\{s_k k, s_p p, s_q q\} = \{1, 1, \sqrt{2}\}$, the solution is

$$u^{s_k}(\boldsymbol{k}, t) = 1\,, \quad u^{s_p}(\boldsymbol{p}, t) = 1\,, \quad u^{s_q}(\boldsymbol{q}, t) = 0\,. \tag{C1}$$

Thus, the period is $\mathcal{T}_{\{1,1,\sqrt{2}\}} = +\infty$ for both real and complex systems.

(2) For the triad interactions $\{1, -\sqrt{2}, -1\}$, $\{1, -\sqrt{2}, \sqrt{3}\}$, and $\{1, -\sqrt{2}, -\sqrt{3}\}$, the initial values of $u^{s_k}(\boldsymbol{k})$, $u^{s_p}(\boldsymbol{p})$, and $u^{s_q}(\boldsymbol{q})$ are 1, 0.5, and 0, respectively. The equations of complex argument and modulus [Eq. (A3)] are analyzed. Particular solutions to the complex argument equations take the form

$$\theta_{s_k}(\boldsymbol{k}, t) = 0\,, \quad \theta_{s_p}(\boldsymbol{p}, t) = 0\,, \quad \theta_{s_q}(\boldsymbol{q}, t) = \theta_g, \tag{C2}$$

regardless of values of $|u^{s_k}|(\boldsymbol{k}, t)$, $|u^{s_p}|(\boldsymbol{p}, t)$, and $|u^{s_q}|(\boldsymbol{q}, t)$. Consequently, the modulus equations can be rewritten as

$$\begin{aligned}
\frac{\partial |u^{s_k}|(\boldsymbol{k}, t)}{\partial t} &= (s_p p - s_q q)|g||u^{s_p}|(\boldsymbol{p}, t)|u^{s_q}|(\boldsymbol{q}, t),\\
\frac{\partial |u^{s_p}|(\boldsymbol{p}, t)}{\partial t} &= (s_q q - s_k k)|g||u^{s_q}|(\boldsymbol{q}, t)|u^{s_k}|(\boldsymbol{k}, t),\\
\frac{\partial |u^{s_q}|(\boldsymbol{q}, t)}{\partial t} &= (s_k k - s_p p)|g||u^{s_k}|(\boldsymbol{k}, t)|u^{s_p}|(\boldsymbol{p}, t),
\end{aligned} \tag{C3}$$

which have the same forms as Eq. (7) in the real field. As pointed out by Ref. 8, the prefactors g of a triad interaction have the same modulus in different helical coordinate systems. Therefore, the period of modulus dynamics, which indicates the period of energy transfer, is the same as that in the real field.

(3) For the triad interaction $\{1, 1, -\sqrt{2}\}$, Eq. (7) can be rewritten as

$$\begin{aligned}
\dot{u}^{s_k}(\boldsymbol{k}, t) &= g(s_p p - s_q q)\bar{u}^{s_p}(\boldsymbol{p}, t)\bar{u}^{s_q}(\boldsymbol{q}, t),\\
\dot{u}^{s_p}(\boldsymbol{p}, t) &= g(s_q q - s_k k)\bar{u}^{s_q}(\boldsymbol{q}, t)\bar{u}^{s_k}(\boldsymbol{k}, t),\\
\dot{u}^{s_q}(\boldsymbol{q}, t) &= 0.
\end{aligned} \tag{C4}$$

We can infer from Eq. (C4) that $u^{s_q}(\boldsymbol{q}, t)$ is constant and the second-order derivatives of $u^{s_k}(\boldsymbol{k}, t)$ and $u^{s_p}(\boldsymbol{p}, t)$ are, respectively,

$$\begin{aligned}
\ddot{u}^{s_k}(\boldsymbol{k}, t) &= -(s_p p - s_q q)^2|g|^2|u^{s_q}(\boldsymbol{q})|^2 u^{s_k}(\boldsymbol{k}, t)\,,\\
\ddot{u}^{s_p}(\boldsymbol{p}, t) &= -(s_p p - s_q q)^2|g|^2|u^{s_q}(\boldsymbol{q})|^2 u^{s_p}(\boldsymbol{p}, t)\,.
\end{aligned}$$

Hence, the general solution for $u^{s_k}(\boldsymbol{k}, t)$ is

$$u^{s_k}(\boldsymbol{k}, t) = C_1 e^{\mathrm{i}\omega t} + C_2 e^{-\mathrm{i}\omega t}, \tag{C5}$$

where C_1 and C_2 are complex constants and $\omega = |s_p p - s_q q| \cdot |g| \cdot |u^{s_q}(\boldsymbol{q})|$. As a consequence, $|u^{s_k}(\boldsymbol{k}, t)|^2 = |C_1|^2 + |C_2|^2 + 2\mathrm{Re}(C_1\overline{C_2}e^{\mathrm{i}2\omega t})$, where $\mathrm{Re}(\bullet)$ stands for the real part. Thus, the period of energy transfer is

$$\mathcal{T}_{\{1,1,-\sqrt{2}\}} = \frac{2\pi}{2\omega} = \frac{\pi}{|s_p p - s_q q||g||u^{s_q}(\boldsymbol{q})|}\,,$$

which is the same as Eq. (11).

In brief, for these typical triad interactions, the periods of energy exchange among complex modes are the same as those in the real case.

APPENDIX D: THE CASE OF $a^2 = b^2$ IN SEC. II B

When $a^2 = b^2$, which corresponds to the case that $H = s_k kT$, i.e., $(s_k k - s_p p)|u^{s_p}|^2 = (s_k k - s_q q)|u^{s_q}|^2$, the integral (14) can be rewritten as

$$\int_{u_0^{s_k}}^{u^{s_k}(t)} \frac{du}{a^2 - u^2} = \pm g\sqrt{(s_k k - s_q q)(s_p p - s_k k)}\, t. \tag{D1}$$

The solutions can be expressed via hyperbolic functions as

$$\begin{aligned}
u^{s_k}(\boldsymbol{k}) &= \pm\sqrt{\frac{s_q qT - H}{s_q q - s_k k}}\tanh\left(g\sqrt{(s_k k - s_q q)(s_p pT - H)}(t - t_0)\right),\\
u^{s_p}(\boldsymbol{p}) &= \pm\sqrt{\frac{s_q qT - H}{s_q q - s_p p}}\,\mathrm{sech}\left(g\sqrt{(s_k k - s_q q)(s_p pT - H)}(t - t_0)\right),\\
u^{s_q}(\boldsymbol{q}) &= \pm\sqrt{\frac{s_p pT - H}{s_p p - s_q q}}\,\mathrm{sech}\left(g\sqrt{(s_k k - s_q q)(s_p pT - H)}(t - t_0)\right),
\end{aligned} \tag{D2}$$

where

TABLE II. Information of the first 15 modal terms.

Mode number (n)	Modal frequency (k_n)	Modal amplitude (A_n)	Magnitude of amplitude ($\lvert A_n \rvert$)
1	3.285 34 − 5.809 44i	12.461 24 + 14.056 14i	18.784 50
2	−3.285 34 − 5.809 44i	12.461 24 − 14.056 14i	18.784 50
3	−5.518 75 − 4.086 57i	−6.166 20 + 3.633 58i	7.157 16
4	5.518 75 − 4.086 57i	−6.166 20 − 3.633 58i	7.157 16
5	−1.811 97 − 2.305 34i	−5.354 57 − 0.426 53i	5.371 53
6	1.811 97 − 2.305 34i	−5.354 57 + 0.426 53i	5.371 53
7	−8.786 30 − 4.643 47i	−0.677 22 − 0.608 09i	0.910 16
8	8.786 30 − 4.643 47i	−0.677 22 + 0.608 09i	0.910 16
9	−0.640 33i	0.464 66	0.464 66
10	29.138 67 − 29.785 25i	0.008 70 − 0.012 23i	0.015 01
11	−29.138 67 − 29.785 25i	0.008 70 + 0.012 23i	0.015 01
12	−13.722 17 − 2.176 33i	−0.000 91 − 0.013 40i	0.013 43
13	13.722 17 − 2.176 33i	−0.000 91 + 0.013 40i	0.013 43
14	16.903 54 − 2.214 98i	−0.001 77 + 0.005 91i	0.006 17
15	−16.903 54 − 2.214 98i	−0.001 77 − 0.005 91i	0.006 17

TABLE III. Information of the first 8 modal terms of e(20).

Mode number (n)	Modal frequency (k_n)	Modal amplitude (A_n)	Magnitude of amplitude ($\lvert A_n \rvert$)
1	−11.283 51i	0.007 65	0.007 65
2	11.070 94 − 9.973 20i	0.002 15 + 0.003 45i	0.004 06
3	−11.070 94 − 9.973 20i	0.002 15 − 0.003 45i	0.004 06
4	−1.415 97i	0.002 09	0.002 09
5	18.728 54 − 2.862 15i	0.001 12 + 0.001 51i	0.001 87
6	−18.728 54 − 2.862 15i	0.001 12 − 0.001 51i	0.001 87
7	21.169 06 + 0.333 25i	0.000 20 + 0.000 13i	0.000 24
8	−21.169 06 + 0.333 25i	0.000 20 − 0.000 13i	0.000 24

$$t_0 = \mp \frac{1}{g\sqrt{(s_p p T - H)(s_k k - s_q q)}} \tanh^{-1}\left(\sqrt{\frac{s_q q - s_k k}{s_q q T - H}} u_0^{s_k}(\boldsymbol{k})\right),$$

with $u_0^{s_k}(\boldsymbol{k})$ the initial value of $u^{s_k}(\boldsymbol{k})$, and the sign of each equation is determined by initial conditions. In this case, the solutions are not periodic any more.

APPENDIX E: PRONY DECOMPOSITIONS

The first 15 modal terms of $e(1)$ in the case of the local triad interaction and the first 8 modal terms of $e(20)$ in the case of the nonlocal triad interaction, including complex frequencies k_n and complex amplitudes A_n, are listed, respectively, in Tables II and III. For $e(1)$, the period of the dominant mode (mode 1 or 2) reads $\mathcal{T} = \frac{2\pi}{3.28534} = 1.912\,5$. However, for $e(20)$, the first modal term is a purely decaying signal, and the period of the dominant mode (mode 2 or 3) reads $\mathcal{T} = \frac{2\pi}{11.07094} = 0.567\,5$. The comparisons between the original and reconstructed signals, $e(1)$ and $e(20)$, are shown in Figs. 7 and 8, respectively.

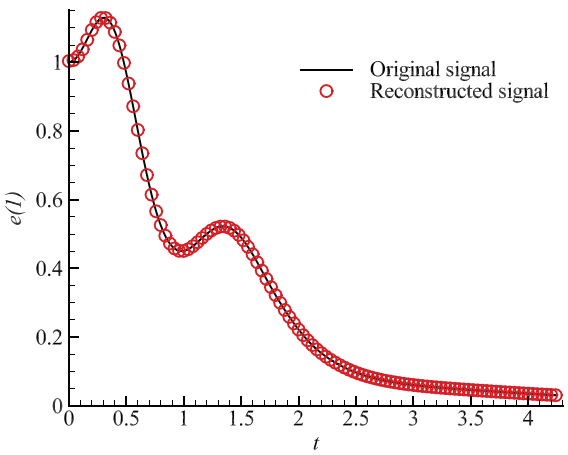

FIG. 7. Original and reconstructed signals of $e(1)$.

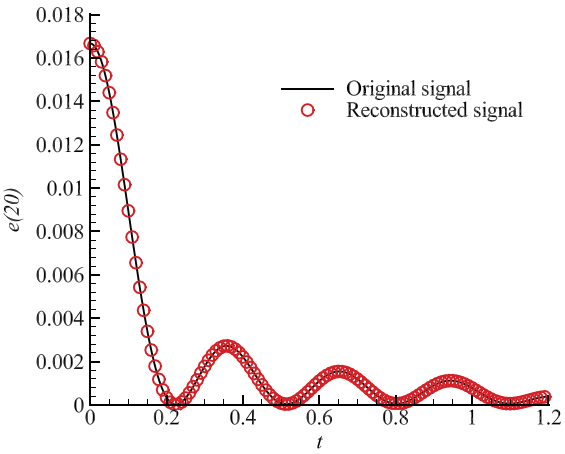

FIG. 8. Original and reconstructed signals of $e(20)$.

DATA AVAILABILITY

The data that support the findings of this study are available from the corresponding author upon reasonable request.

REFERENCES

[1]A. N. Kolmogorov, "The local structure of turbulence in incompressible viscous fluid for very large Reynolds number," Proc. R. Soc. A **30**, 301 (1941).
[2]L. S. G. Kovasznay, "The spectrum of locally isotropic turbulence," Phys. Rev. **73**, 1115–1116 (1948).
[3]J. C. Vassilicos, "Dissipation in turbulent flows," Annu. Rev. Fluid Mech. **47**, 95–114 (2015).
[4]Y. Zhou, "Interacting scales and energy transfer in isotropic turbulence," Phys. Fluids **5**, 2511–2524 (1993).
[5]P. K. Yeung and Y. Zhou, "Universality of the Kolmogorov constant in numerical simulations of turbulence," Phys. Rev. E **56**(2), 1746–1752 (1997).
[6]R. H. Kraichnan, "Inertial ranges in two-dimensional turbulence," Phys. Fluids **10**(7), 1417–1423 (1967).
[7]R. H. Kraichnan, "Helical turbulence and absolute equilibrium," J. Fluid Mech. **59**, 745–752 (1973).
[8]F. Waleffe, "The nature of triad interactions in homogeneous turbulence," Phys. Fluids A **4**(2), 350–363 (1992).
[9]S. A. Orszag, "Approximate calculation of the Kolmogorov–Obukhov constant," Phys. Fluids **10**(2), 454–455 (1967).
[10]T. Pestana and S. Hickel, "Rossby-number effects on columnar eddy formation and the energy dissipation law in homogeneous rotating turbulence," J. Fluid Mech. **885**, A7 (2020).
[11]S. A. Orszag, *Lectures on the Statistical Theory of Turbulence*, edited by R. Balian and J. L. Peube (Gordon and Breach, New York, 1974).
[12]F. Liu, L. P. Lu, W. J. T. Bos, and L. Fang, "Assessing the non-equilibrium of decaying turbulence with reversed initial fields," Phys. Rev. Fluids **4**, 084603 (2019).
[13]L. Fang, T. Wu, and W. J. T. Bos, "Staircase scaling of short-time energy transfer in turbulence," J. Turbul. **21**(4), 234–242 (2020).
[14]J. Chai, T. Wu, and L. Fang, "Single-scale two-dimensional-three-component generalized-Beltrami-flow solutions of incompressible Navier–Stokes equations," Phys. Lett. A **384**, 126857 (2020).
[15]W. Heisenberg, "On the statistical theory of turbulence," Z. Phys. **124**, 628–657 (1948).
[16]G. Comte-Bellot and S. Corrsin, "Simple Eulerian time correlation of full- and narrow-band velocity signals in grid-generated, isotropic turbulence," J. Fluid Mech. **48**(2), 273–337 (1971).
[17]C. Bailly and G. Comte-Bellot, *Turbulence* (Springer, 2015).
[18]L. Onsager, "The distribution of energy in turbulence," Phys. Rev. **68**, 286 (1945).
[19]L. Onsager, "Statistical hydrodynamics," Nuovo Cimento **6**(suppl), 279–287 (1949).
[20]C. F. Weizsäcker, "Das spectrum der turbulenz bei grossen Reynoldsschen zahlen," Z. Phys. **124**, 614–627 (1948).
[21]P. Constantin and A. Majda, "The Beltrami spectrum for incompressible fluid flows," Commun. Math. Phys. **115**, 435–456 (1988).
[22]L. Biferale, S. Musacchio, and F. Toschi, "Split energy-helicity cascades in three-dimensional homogeneous and isotropic turbulence," J. Fluid Mech. **730**, 309–327 (2013).
[23]H. K. Moffatt, "Note on the triad interactions of homogeneous turbulence," J. Fluid Mech. **741**(2), 106–124 (2014).
[24]M. D. Bustamante and E. Kartashova, "Resonance clustering in wave turbulent regimes: Integrable dynamics," Commun. Comput. Phys. **10**, 1211–1240 (2011).
[25]M. D. Bustamante and E. Kartashova, "Effect of the dynamical phases on the nonlinear amplitudes' evolution," Europhys. Lett. **85**, 34002 (2009).
[26]M. Lesieur, *Turbulence in Fluids* (Springer, 2008).
[27]L. Fang, L. Shao, J. P. Bertoglio, G. Cui, C. Xu, and Z. Zhang, "An improved velocity increment model based on Kolmogorov equation of filtered velocity," Phys. Fluids **21**(6), 065108 (2009).
[28]W. J. T. Bos and J. P. Bertoglio, "Dynamics of spectrally truncated inviscid turbulence," Phys. Fluids **18**, 071701 (2006).
[29]J. A. Domaradzki and R. S. Rogallo, "Local energy transfer and nonlocal interactions in homogeneous, isotropic turbulence," Phys. Fluids A **2**(3), 413–426 (1990).
[30]V. Borue and S. A. Orszag, "Local energy flux and subgrid-scale statistics in three-dimensional turbulence," J. Fluid Mech. **366**, 1–31 (1998).
[31]R. Stepanov and F. Plunian, "Systematic bias in the calculation of spectral density from a three-dimensional spatial grid," Phys. Rev. E **90**, 053309 (2014).
[32]R. Prony, "Essai experimental et analytique sur les lois de la dilatabilite des fluides elastiques, et sur celles de la force expansive de la vapeur de l'eau et de la vapeur de l'alkool, a differentes temperatures," J. L'ecole Polytech. **1**, 24–76 (1795).
[33]A. S. Householder, "On Prony's method of fitting exponential decay curves and multiple-hit survival curves," Report No. ORNL-455, Oak Ridge National Laboratory, 1950.
[34]W. J. T. Bos and R. Rubinstein, "Dissipation in unsteady turbulence," Phys. Rev. Fluids **2**, 022601 (2017).
[35]P. F. Yang, A. Pumir, and H. T. Xu, "Generalized self-similar spectrum and the effect of large-scale in decaying homogeneous isotropic turbulence," New J. Phys. **20**, 103035 (2018).
[36]G. C. Layek Sunita, "Non-Kolmogorov dissipation in a turbulent planar jet," Phys. Rev. Fluids **3**, 124605 (2018).
[37]M. Buzzizotti, B. P. Murray, L. Biferale, and M. D. Bustamante, "Phase and precession evolution in the burgers equation," Eur. Phys. J. E **39**(3), 34 (2016).
[38]B. P. Murray and M. D. Bustamante, "Energy flux enhancement, intermittency and turbulence via Fourier triad phase dynamics in the 1-D burgers equation," J. Fluid Mech. **850**, 624–645 (2018).